NUMERICAL ANALYSIS OF PEELING-BALLOONING STABILITY AT VARIOUS TRIANGULARITIES IN GLOBUS-M2

[1,2]V.V. SOLOKHA, [1]I.M. BALACHENKOV, [1]V.K. GUSEV, [1]G.S. KURSKIEV, [1]E.O. KISELEV, [1]V.B. MINAEV, [1]A.N. NOVOKHATSKY, [1,2]V.D. PETRENKO, [1]Y.V. PETROV, [1]N.V. SAKHAROV, [1]P.B. SHCHEGOLEV, [1,2]K.D. SHULYATIEV, [1,2]A.Y. TELNOVA, [1]E.E. TKACHENKO, [1]S.Y. TOLSTYAKOV, [1]V.I. VARFOLOMEEV, [1,2]N.S. ZHILTSOV
[1]Ioffe Institute, St. Petersburg, Russian Federation
[2]Peter the Great Polytechnic University, St. Petersburg, Russian Federation
Email: vsolokha@mail.ioffe.ru

A.A. KAVIN
JSC «NIIEFA»
St. Petersburg, Russian Federation

A.M. PONOMARENKO, A.Y. TOKAREV, A.Y. YASHIN
Peter the Great St. Petersburg Polytechnic University
St. Petersburg, Russian Federation

Abstract

The goal of the Globus-M2 tokamak is to operate in conditions of high ion temperatures and corresponding steep edge plasma pressure profiles. The high-performance regimes with steep pressure are characterized by the edge-localized instabilities leading to increased heat loads on plasma-facing components. Plasma shaping conditions were shown to have a remarkable influence on the edge plasma stability, and in this work we performed a series of the three-field magnetohydrodynamic simulations using BOUT++ code in order to investigate the impact of the plasma shape on the edge stability in Globus-M2 plasmas. Different triangularities ranging from 0.19 to 0.40 were considered. The low triangularity equilibria were characterized by lower values of safety factor and magnetic shear than high triangularity equilibria, leading to a relatively low marginal stability boundary at approximately 1 kPa and the spatial mode structure located at the separatrix, indicating a significant peeling mode contribution. The medium triangularity case was characterized by a significantly steeper marginal stability boundary at approximately 2.5 kPa, high toroidal mode numbers of the unstable mode, and top of the pedestal localization indicating the ballooning properties and explaining the experimentally observable difference in critical pressures.

INTRODUCTION

The formation of the reduced transport region during the high confinement mode operation (H-mode) implies steep density and temperature profiles, which drive the development of edge localized modes (ELMs). They are observable as periodic abrupt plasma losses to open field lines leading to increased heat loads on plasma-facing components. Plasma shaping conditions were shown to have a remarkable influence on the edge plasma stability in conventional [1] as well as spherical [2] tokamaks. The compact spherical tokamak Globus-M2 [3] was shown to be able to achieve hot-ion H-mode with remarkable high ion temperature and moderate electron temperature and density. Despite high edge plasma pressure, ELMs obtain type-V traits at pedestal pressures higher than p_{ped}= 4 kPa in discharges using external power input provided by neutral beam injection. The aforementioned discharges have an intrinsically high value of triangularity (δ) around 0.4 and elongation (κ) around 1.9. Experiments with medium triangularity values (δ=0.3) showed the presence of ELMs at p_{ped}= 2 kPa. The recent observation [4] of the shaping influence on the peeling-ballooning destabilization exhibited ELMs onsets at low pressure (p_{ped}= 1.2 kPa) in magnetic configuration with triangularity around 0.2 and the elongation around 1.9. The decrease of the triangularity leads to the expansion of plasma volume located at the bad curvature region. Also, the important feature of low triangularity discharges in comparison with high triangularity discharges was having 20% lower magnetic shear values at virtually the same value of safety factor. The H-mode discharge with variable triangularity from 0.18 to 0.21 has shown the 20% increase in critical pedestal pressure corresponding to the type-V ELMy phase. The previously conducted simulations using BOUT++ code [5] exhibited the intrinsically unstable peeling–ballooning mode with low toroidal numbers (n ~ 5) in low triangularity Globus-M2 discharges.

However, while the triangularity was shown to be an important plasma parameter in terms of peeling-ballooning stability, the static triangularity comparison was complicated due to the operation limits of the Globus-M2 electromagnetic system. To overcome the hardware limitations and explore the parameter space of the Globus-M2 tokamak, the numerical study of the peeling-ballooning mode was conducted.

NUMERICAL RESULTS

1.1. Magnetic configurations

The investigation of peeling-ballooning stability was performed on a set of magnetic equilibria provided by free-boundary plasma equilibrium codes FreeGS [6], pyGSS [7], and PET [8] for Globus-M2 configurations with triangularities ranging from 0.19 to 0.40, while having the same elongation. Last closed magnetic surfaces for discharges with toroidal magnetic field B_T = 0.7 T and plasma current I_P = 0.3 MA are shown in Fig. 1.

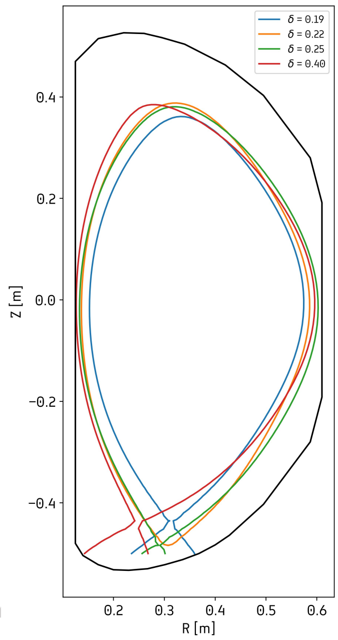

FIG. 1. Set of Globus-M2 magnetic configurations with various triangularities δ∈[0.19, 0.40].

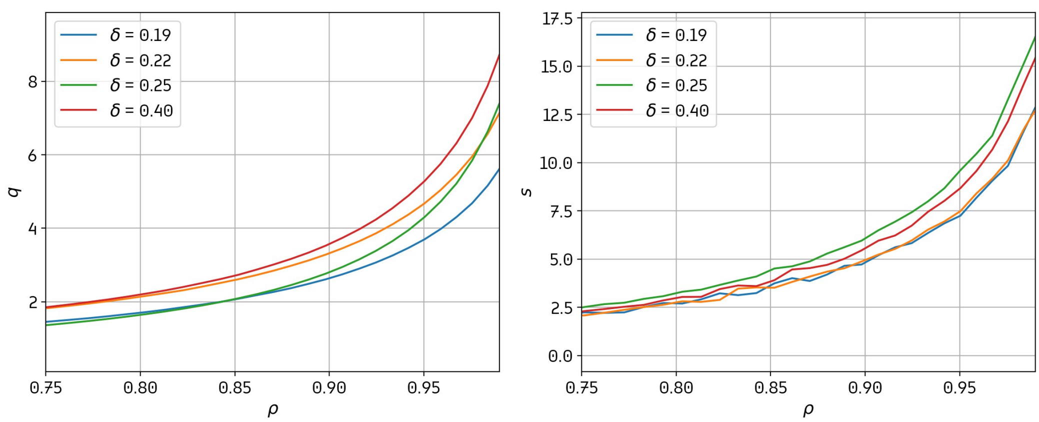

FIG. 2. Profiles of safety factor (left) and magnetic shear (right) for Globus-M2 magnetic configurations with various triangularities δ∈[0.19, 0.40].

The safety factor and magnetic shear exhibit a significant difference for various triangularities. The low triangularity equilibria have the lowest values of the safety factor, leading to more unstable discharges experimentally than discharges with high triangularity. On the other hand, a decrease of safety factor values leads to a lower normalized pressure gradient, which can have a stabilization effect on the ballooning mode. However, the magnetic shear decrease might lead to approaching a peeling boundary limit with a decrease of the triangularity.

1.2. Peeling-ballooning mode simulations

The quantitative estimations of the peeling-ballooning stability of the Globus-M2 edge tokamak plasmas were carried out by the BOUT++ code. The solution of single-fluid magnetohydrodynamic equations was done by the finite difference method in the three-dimensional tokamak geometry. The three-field model was used with the inclusion of the diamagnetic effect. The diamagnetic effect is known to have a stabilizing effect on the ideal ballooning modes in the edge pedestal with a growth rate below half of the ion diamagnetic frequency [9]. The importance of the diamagnetic term is highlighted in spherical tokamaks, as the toroidal magnetic field is usually below 1 T and ion temperatures are around the 0.5 keV level, leading to a large Larmor radius relative to the pedestal width, resulting in a decrease of the toroidal numbers of the most unstable mode. The linear calculations were performed with the low plasma resistivity assumption with a Lundquist number of $S=10^8$. The hyper resistivity and compression effects were omitted. In the poloidal direction the 0.75-0.97 normalized flux span was covered by the mesh. The mesh with a 64×64 cell resolution in radial and poloidal directions was constructed based on the generated magnetic equilibria.

The initial plasma pressure profile was introduced by a hyperbolic tangent parameterized by its height and width (Fig. 3). The current density profile consisted of two components: ohmic and bootstrap components. The Ohmic component of the current density was estimated by the ASTRA [10] simulations for equivalent Globus-M2 discharges to be equal to 0.2 - 0.3 MA/m². The bootstrap current was estimated using the Sauter analytical formula [11]. However, the current gradients due to the bootstrap current are significantly larger than the non-uniformity of the Ohmic current density; therefore, the Ohmic component was assumed to be spatially constant. The pedestal stability analysis was performed by means of pedestal stability diagrams, which depict the dependence of the peeling–ballooning mode growth rate on the height and width of the pedestal. The diagram was calculated using the set of simulations for each pedestal height and width. The growth rate of the peeling–ballooning mode for each simulation was estimated from the root mean square pressure perturbation at the low-field side midplane point. The assessment of the growth rate allowed to compare conditions corresponding to edge-localized mode bursts and growth rate yielding the critical value of 0.1 inverse Alfven times; the estimation was inferred by the condition of the current sheet scale to be larger than the scale of the ion Larmor radius.

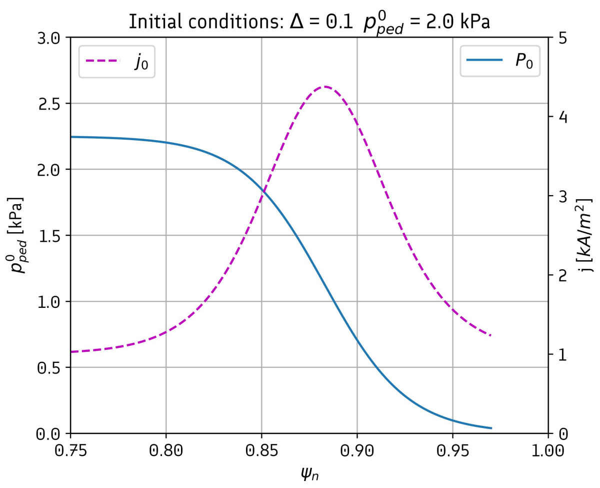

FIG. 3. Example of the initial conditions for the case with pedestal width of 0.1 and height of 2.0 kPa.

Peeling-ballooning stability calculations for low triangularity equilibria corresponding to the toroidal magnetic field B_T = 0.7 T, plasma current I_P = 0.3 MA and triangularity δ=0.19 are shown in Fig. 4. For experimental values of the pedestal width around 0.08, the critical pressure is around 1 kPa, as was observed previously, the peeling-ballooning mode is expected to become unstable. However, the widening of the pedestal does not allow increasing pedestal height beyond 1.25 kPa levels.

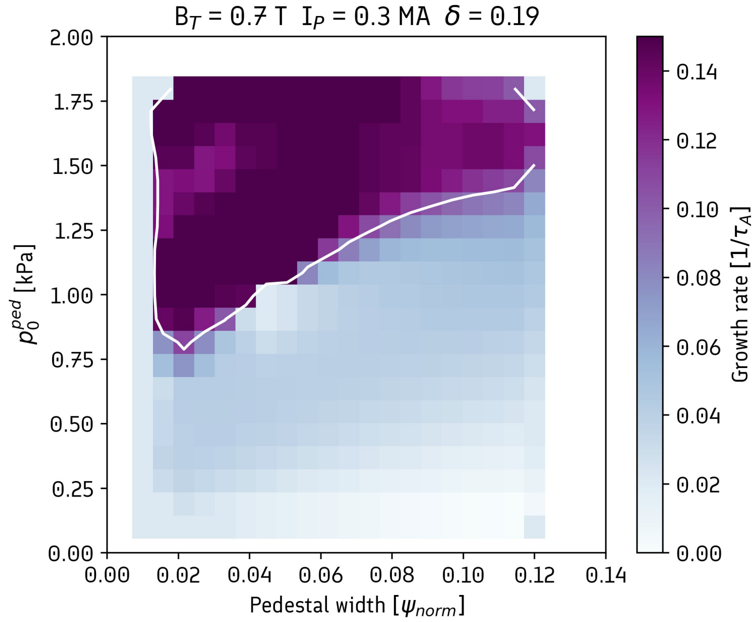

FIG. 4. Peeling-ballooning growth rate dependency on the pedestal width and height for the case with B_T = 0.7 T, I_P = 0.3 MA, and δ=0.19.

The 10% raise in triangularity leads to a significant flattening of the marginal stability boundary (Fig. 5). Despite the increase in critical pressure value by 15% for experimentally relevant pedestal width, the further flattening of the stability boundary indicates the significant influence of peeling mode on the edge plasma stability.

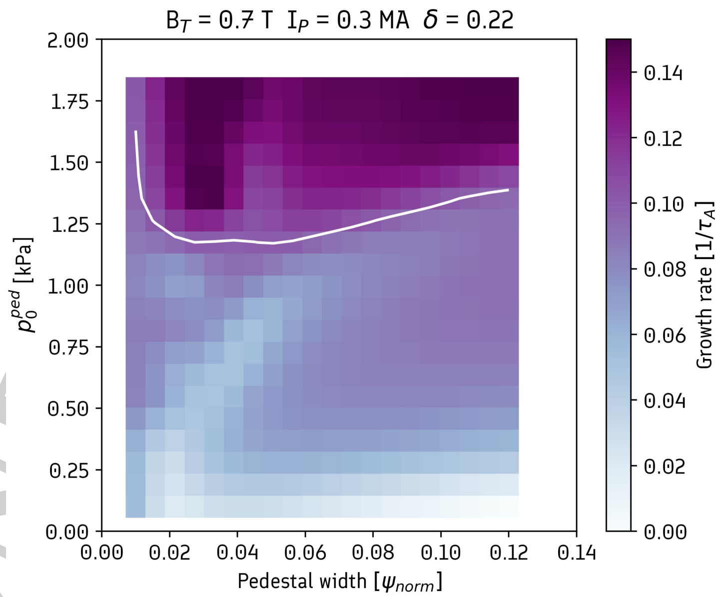

FIG. 5. Peeling-ballooning growth rate dependency on the pedestal width and height for the case with B_T = 0.7 T, I_P = 0.3 MA, and δ=0.22.

However, the further increase in triangularity leads to a raise of the peeling-ballooning stability boundary (Fig. 6). The case with medium triangularity δ=0.30 shows up to 3 times higher critical pressures; for the experimentally relevant pedestal width, the critical pressure was found to be approximately 2.3 kPa, which is consistent with the experimental results shown previously. Also, the medium triangularity marginal stability boundary exhibits the steep shape, indicating more pronounced ballooning-type behavior.

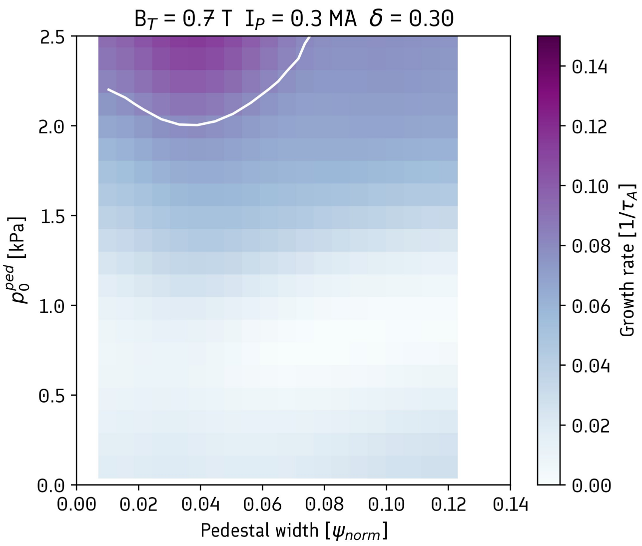

FIG. 6. Peeling-ballooning growth rate dependency on the pedestal width and height for the case with B_T = 0.7 T, I_P = 0.3 MA, and δ=0.30.

The investigation of the spatial mode structure for the low triangularity case (Fig. 7) demonstrated the mode localization in the vicinity of the separatrix with mostly intermediate toroidal mode numbers. It indicates that reduced shear might have caused the significant peeling mode destabilization. But the significant span inside the pedestal and intermediate toroidal mode numbers marks a perceptible ballooning mode contribution.

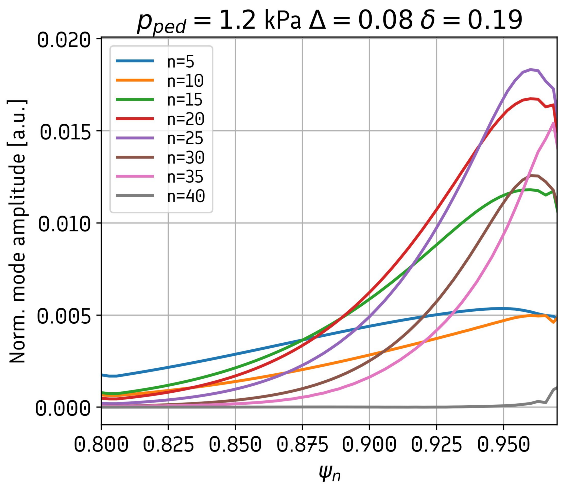

FIG. 7. The spatial structure of toroidal modes normalized amplitudes for the case with B_T = 0.7 T, I_P = 0.3 MA and δ=0.19.

The spatial mode structure for the medium triangularity case (Fig. 8) exhibits highly notable ballooning properties, as the one mode with n=25 is dominating in the simulations. Increased values of the magnetic shear in the medium triangularity case were enough to stabilize the peeling mode branch, and it requires the additional pressure gradient to destabilize the ballooning branch of the peeling-ballooning mode despite the increased values of the safety factor.

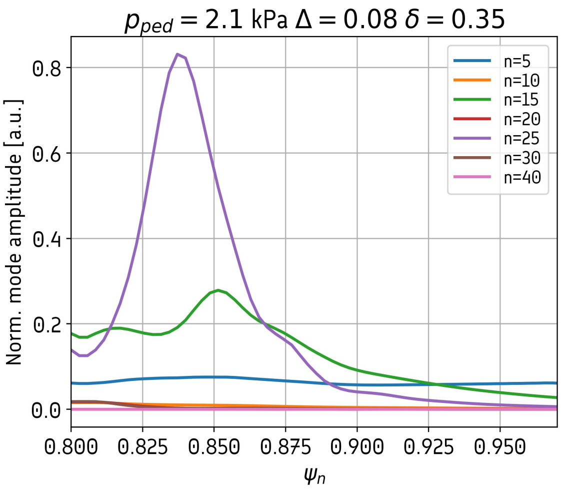

FIG. 8. The spatial structure of toroidal modes normalized amplitudes for the case with B_T = 0.7 T, I_P = 0.3 MA, and δ=0.35.

CONCLUSIONS

In this work we performed a series of the three-field magnetohydrodynamic simulations using BOUT++ code in order to investigate the impact of the plasma shape on the edge stability in Globus-M2 plasmas. Different triangularities ranging from 0.19 to 0.40 were considered. The low triangularity equilibria were characterized by lower values of safety factor and magnetic shear than high triangularity equilibria.

For low triangularity cases, we found a relatively low marginal stability boundary at approximately 1 kPa with a weak dependency on the pedestal width, indicating a significant peeling mode contribution. The spatial mode structure for these cases was located in the vicinity of the separatrix and demonstrated intermediate toroidal numbers of unstable modes. The medium triangularity case was characterized by a significantly steeper marginal stability boundary at approximately 2.5 kPa. The spatial mode structure demonstrated high toroidal mode numbers and top-of-the-pedestal localization of the mode, indicating the ballooning properties of the mode and explaining experimentally observable differences in critical pressures.

ACKNOWLEDGEMENTS

The work was carried out with support by Russian Science Foundation Project 23-72-00024. The experimental data for equilibrium reconstruction utilized the diagnostic measurements supported by project FFUG-2024-0028.

REFERENCES

[1] ZOHM, H., Edge localized modes (ELMs), Plasma Phys. Controlled Fusion 38, 105 (1996).

[2] IMADA, K., et al., Observation of a new pedestal stability regime in MAST Upgrade H-mode plasmas, Nucl. Fusion 64, 086002 (2024).

[3] MINAEV V., et al., Spherical tokamak Globus-M2: Design, integration, construction, Nucl. Fusion 57, 066047 (2017).

[4] SOLOKHA V., et al., Observation of peeling-ballooning destabilization at low pressures in weakly shaped Globus-M2 discharges, Phys. Plasmas 32, 052505 (2025).

[5] DUDSON B., et al., BOUT++: A framework for parallel plasma fluid simulations, Comput. Phys. Commun. 180, 1467–1480 (2009).

[6] JEON Y.M., et al., Development of a free-boundary tokamak equilibrium solver for advanced study of tokamak equilibria, J. Korean Phys. Soc. 67, 843 (2015).

[7] KISELEV E., et al., Free-Boundary Plasma Equilibrium Computation in Spherical Globus-M2 Tokamak by Means of the pyGSS Code, Plasma Physics Reports, 49, 1560 (2023).

[8] GALKIN S. A., et al., Comparison of tokamak axisymmetric mode growth rates from linear MHD and equilibrium evolution approaches, Nucl. Fusion 37, 1455 (1997).

[9] ROGERS B. N. and DRAKE J. F., Diamagnetic stabilization of ideal ballooning modes in the edge pedestal, Phys. Plasmas 6, 2797 (1999).

[10] RYTER F., et al., Electron heat transport in ASDEX-Upgrade: Experiment and modelling, Nucl. Fusion 43, 1396 (2003).

[11] SAUTER, O., et al., Neoclassical conductivity and bootstrap current formulas for general axisymmetric equilibria and arbitrary collisionality regime, Phys. Plasmas 6, 2834–2839 (1999)